

Dependence of thermal properties on crystallization behaviors of $(1 - x)\text{MgSiO}_3$ – $x\text{CaMgSi}_2\text{O}_6$ glass-ceramics

Won Jae Yeo, Chang Jun Jeon, Eung Soo Kim *

Department of Materials Engineering, Kyonggi University, Suwon 443-760, South Korea

Available online 26 May 2011

Abstract

Effects of crystallization behaviors on thermal properties of $(1 - x)\text{MgSiO}_3$ – $x\text{CaMgSi}_2\text{O}_6$ ($0.36 \leq x \leq 0.90$) glass-ceramics were investigated. The crystallization behaviors of glasses were confirmed from the activation energy of crystallization (E_a), crystallite size (L) and crystalline phases of clino-enstatite (MgSiO_3) and diopside ($\text{CaMgSi}_2\text{O}_6$). The specific heat capacity of the specimens sintered at 800 °C for 5 h was affected by the E_a of glasses. The thermal conductivity and thermal diffusivity of the sintered specimens were dependent on the L of glass-ceramics. The temperature dependence of thermal conductivity was also discussed for the application of lighting-emitting diode (LED) package and substrate materials.

© 2011 Elsevier Ltd and Techna Group S.r.l. All rights reserved.

Keywords: B. X-ray methods; C. Thermal conductivity; D. Glass ceramics; E. Substrates

1. Introduction

For various industrial applications, MgSiO_3 -based glass-ceramics have been widely investigated due to the good mechanical and low loss electrical properties as well as abundant raw materials in glass batches [1,2]. Enstatite is a low temperature modification of MgSiO_3 , which has three types of characteristic structures such as ortho-enstatite, proto-enstatite and clino-enstatite [2]. These structural characteristics of enstatite affect to the degradation of electrical and mechanical properties. Also, the precise stoichiometric composition of enstatite showed the unstable glass and the narrow sintering window due to the rapid formation of liquid phase during firing [3].

It has been reported [4] that the substitution of Ca^{2+} with different ionic size for Mg^{2+} induced the formation of a more stable diopside ($\text{CaMgSi}_2\text{O}_6$) structure, which improved the electrical and mechanical properties by the reduce of enstatite polymorphism resulted from the substitution of diopside above 12 mol%.

The enstatite–diopside system is one of good candidates available to the package materials for lighting-emitting diodes

(LED) chips in view point of the fast heat dissipations, because this system has relatively low sintering temperature (high sintered density) and high thermal conductivity.

Therefore, the effects of crystallization behaviors on thermal properties of $(1 - x)\text{MgSiO}_3$ – $x\text{CaMgSi}_2\text{O}_6$ glass-ceramics were investigated as a function of $\text{CaMgSi}_2\text{O}_6$ content (x). The activation energy of crystallization, crystallite size and crystalline phases were studied to evaluate the crystallization behaviors of glasses. The temperature coefficient of thermal conductivity (TCK) was also discussed for practical application of LED multilayer devices.

2. Experimental procedures

High-purity oxide powders of CaCO_3 (99%), MgCO_3 (99.9%) and SiO_2 (99.9%) were used as starting powders. The powders were separately prepared according to the desired compositions of MgSiO_3 and $\text{CaMgSi}_2\text{O}_6$, and ground with ZrO_2 balls for 24 h in ethanol. The mixed powders were melted in a platinum crucible at 1500 °C for 3 h and quenched into distilled water. The cullets were pulverized and mixed according to the desired formula of $(1 - x)\text{MgSiO}_3$ – $x\text{CaMgSi}_2\text{O}_6$ ($0.36 \leq x \leq 0.90$), and then melted again at 1500 °C for 3 h. Pure glass frits were obtained by quenching of melts into distilled water. These glass frits were re-milled for 24 h and

* Corresponding author. Tel.: +82 31 249 9764; fax: +82 31 244 6300.

E-mail address: eskim@kyonggi.ac.kr (E.S. Kim).

pressed into pellets isostatically under the pressure of 147 MPa. These pellets were sintered from 750 °C to 950 °C for 5 h in air.

The densities of the sintered specimens were measured by Archimedes method. The differential thermal analysis (DTA) curve was obtained by a simultaneous thermal analyzer-mass spectrometer (STA 409PC-QMS 403C, NETZSCH, Germany) at different heating rates (5–20 K/min). Powder X-ray diffraction analysis (XRD, D/Max-2500V/PC, RIGAKU, Japan) was used to evaluate the crystalline phases and crystallization behaviors of glasses. The thermal properties were measured by a laser flash apparatus (LFA 457, NETZSCH, Germany). The temperature dependence of thermal conductivity was measured in the temperature range from 25 °C to 100 °C.

3. Results and discussion

Fig. 1 shows the differential thermal analysis (DTA) curves of $(1-x)\text{MgSiO}_3$ – $x\text{CaMgSi}_2\text{O}_6$ glass powders heated at a rate of 5 K/min and 0.64MgSiO_3 – $0.36\text{CaMgSi}_2\text{O}_6$ glass powders with different heating rates, respectively. The strong exothermic reactions peaked at 875–914 °C are attributed to the crystallization of glass at each composition and heating rate. For the glasses with same heating rate of 5 K/min (Fig. 1(a)), the peak temperature of crystallization (T_p) was shifted to lower temperature with the $\text{CaMgSi}_2\text{O}_6$ content (x). However, the T_p of glasses with same $\text{CaMgSi}_2\text{O}_6$ content ($x = 0.36$) was shifted to higher temperature with the heating rate (Fig. 1(b)). The similar tendency was confirmed for all glasses with different heating rates. From the T_p of glasses with different heating rates, the activation energy of crystallization (E_a) was calculated using following modified form of Kissinger equation.

$$\ln\left(\frac{T_p^2}{\beta^n}\right) = \left(\frac{E_a}{RT_p}\right) + \text{constant} \quad (1)$$

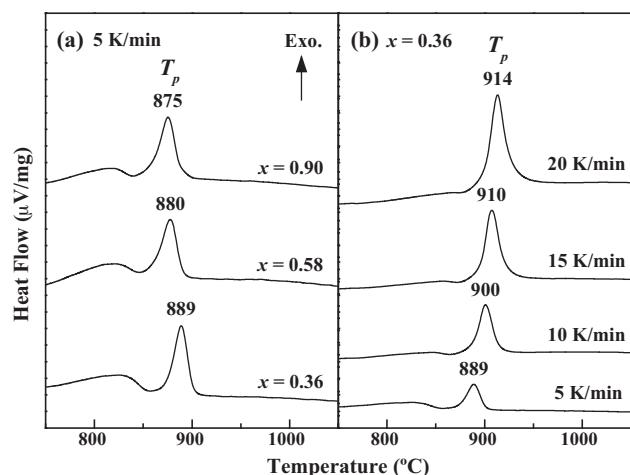


Fig. 1. DTA curves of (a) $(1-x)\text{MgSiO}_3$ – $x\text{CaMgSi}_2\text{O}_6$ glass powders heated at a rate of 5 K/min and (b) 0.64MgSiO_3 – $0.36\text{CaMgSi}_2\text{O}_6$ glass powders with different heating rates.

where β is the heating rate (5–20 K/min), R is the ideal gas constant and n is the Avrami constant, respectively. This equation suggested [5] that nucleation does not occur during crystal growth and crystal growth is interface controlled. In this study, the n value was considered as equal to 1, which is the case for surface crystallization [5] because MgSiO_3 and $\text{CaMgSi}_2\text{O}_6$ generally induced the surface crystallization [6,7]. Therefore, the plots of $\ln(T_p^2/\beta)$ versus $1000/T_p$ for crystallization of $(1-x)\text{MgSiO}_3$ – $x\text{CaMgSi}_2\text{O}_6$ glasses are shown in Fig. 2. The E_a values were obtained from the slope of solid line by least squares fit of the data points. The validity of Kissinger method [8] was supported by the high values of correlation coefficients (R^2). With increasing of $\text{CaMgSi}_2\text{O}_6$ content (x), the E_a of glasses was increased up to $x = 0.58$ and then decreased (Fig. 2).

To investigate the dependence of thermal properties on the crystallization behaviors of $(1-x)\text{MgSiO}_3$ – $x\text{CaMgSi}_2\text{O}_6$ glasses, the sintering temperatures from 750 °C to 950 °C were determined from the results of DTA data. With increasing of sintering temperature from 750 °C to 950 °C, the apparent density of the specimens was remarkably increased up to 800 °C, and then almost constant of 2.9–3.0 g/cm³ through the entire range of compositions. To reduce the effects of density on the thermal properties, the optimal sintering temperature was 800 °C for the highest sintered densities.

Fig. 3 shows the XRD patterns ((a) $2\theta = 10$ – 80° and (b) $2\theta = 29$ – 32°) of $(1-x)\text{MgSiO}_3$ – $x\text{CaMgSi}_2\text{O}_6$ specimens sintered at 750 °C and 800 °C for 5 h. XRD pattern of specimens sintered at 750 °C for 5 h showed the typical amorphous halo (Fig. 3(a)). However, two phases with monoclinic clinostatite (MgSiO_3) and monoclinic diopside ($\text{CaMgSi}_2\text{O}_6$) structures were confirmed for the specimens sintered at 800 °C for 5 h. With increasing of $\text{CaMgSi}_2\text{O}_6$ content (x), the (3 1 0) plane of MgSiO_3 phase was split into the (3 1 0) and ($\bar{3}$ 1 1) planes of $\text{CaMgSi}_2\text{O}_6$ phase at $2\theta = 30$ – 31° (Fig. 3(b)). Also, the full width at half maximum (FWHM) of main peaks was decreased with $\text{CaMgSi}_2\text{O}_6$ content (x). The thermal properties of glass-ceramics are affected by the crystallite size due to the

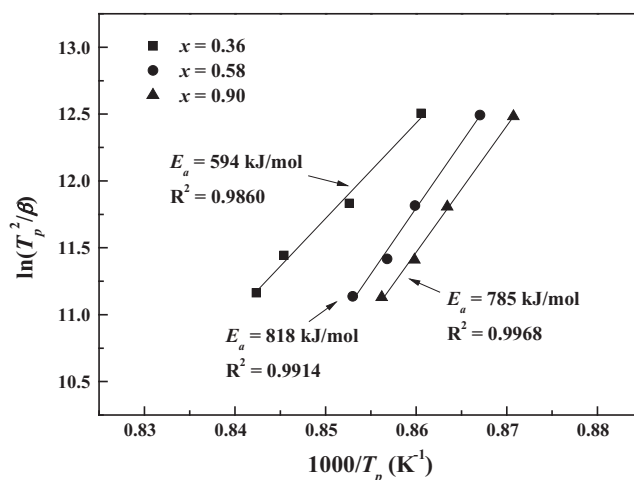


Fig. 2. Plots of activation energy for crystallization (E_a) of $(1-x)\text{MgSiO}_3$ – $x\text{CaMgSi}_2\text{O}_6$ glasses (R^2 : correlation coefficients).

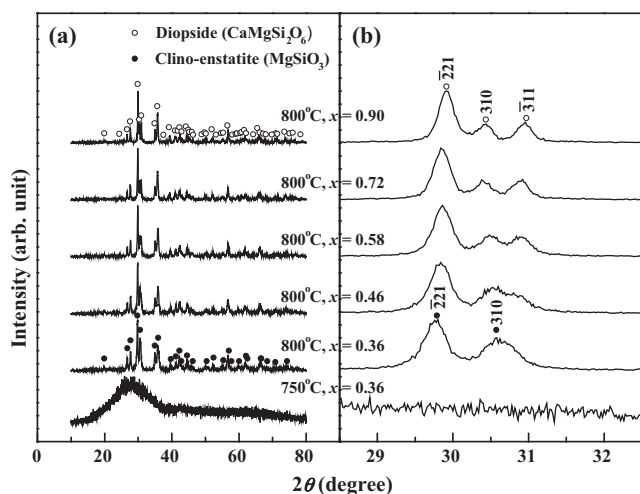


Fig. 3. XRD patterns of $(1-x)\text{MgSiO}_3-x\text{CaMgSi}_2\text{O}_6$ specimens sintered at 750 °C and 800 °C for 5 h; (a) $2\theta = 10\text{--}80^\circ$ and (b) $2\theta = 29\text{--}32^\circ$.

interfacial resistance [9]. Therefore, the average crystallite size (L) of each composition was calculated from the FWHM of peaks with strong intensities at $2\theta = 25\text{--}40^\circ$ of XRD patterns using Scherrer's equation [9].

$$L = \frac{K\lambda}{\beta \cos \theta} \quad (2)$$

where λ is the wavelength of the X-ray radiation ($\lambda = 0.154$ nm), β is the FWHM of the peak (radians) corrected for instrumental broadening, θ is the Bragg angle, and K is a constant related to the crystallite shape (approximately equal to 0.9), respectively. With increasing of $\text{CaMgSi}_2\text{O}_6$ content (x), the L of the specimens sintered at 800 °C for 5 h was increased from 20.08 nm ($x = 0.36$) to 29.68 nm ($x = 0.90$). Based on the XRD patterns of the specimens, the reaction compounds between MgSiO_3 and $\text{CaMgSi}_2\text{O}_6$ were not detected, which in turn, the chemical reactions between MgSiO_3 and $\text{CaMgSi}_2\text{O}_6$ were not observed.

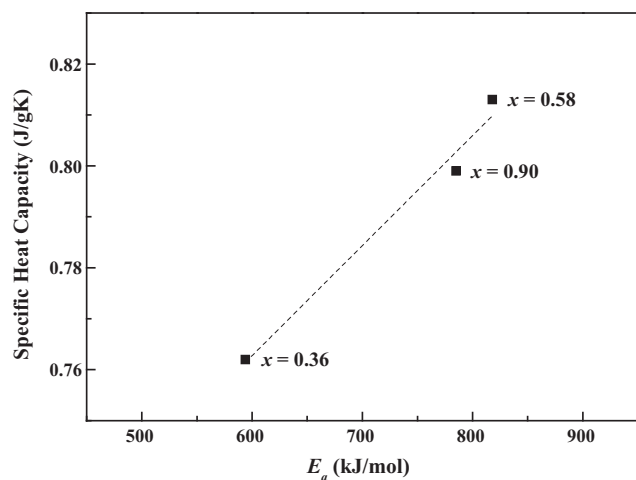


Fig. 4. Dependence of specific heat capacity on activation energy for crystallization (E_a) of $(1-x)\text{MgSiO}_3-x\text{CaMgSi}_2\text{O}_6$ specimens sintered at 800 °C for 5 h.

Fig. 4 shows the dependence of specific heat capacity on E_a of $(1-x)\text{MgSiO}_3-x\text{CaMgSi}_2\text{O}_6$ specimens sintered at 800 °C for 5 h. With increasing of $\text{CaMgSi}_2\text{O}_6$ content (x), the specific heat capacity of the specimens increased up to $x = 0.58$ and then decreased. These results could be attributed to the E_a of $(1-x)\text{MgSiO}_3-x\text{CaMgSi}_2\text{O}_6$ glasses.

Fig. 5 shows the dependence of thermal conductivity and thermal diffusivity on L of $(1-x)\text{MgSiO}_3-x\text{CaMgSi}_2\text{O}_6$ specimens sintered at 800 °C for 5 h. With increasing of $\text{CaMgSi}_2\text{O}_6$ content (x), the thermal conductivity and thermal diffusivity of the specimens were increased due to the decrease of interface area resulted from the increase of L . In general, the thermal conductivity can be determined from thermal diffusivity, specific heat capacity and density. However, the thermal conductivity of materials is largely dependent on the thermal diffusivity than specific heat capacity and density [10]. Therefore, the thermal conductivity of the specimens showed the similar tendency to the thermal diffusivity with the $\text{CaMgSi}_2\text{O}_6$ content (x) in this study.

For the view point of practical application of LED multilayer devices, the change of thermal conductivity with temperature is a very important factor to dissipate the heat effectively, which could be evaluated by the temperature coefficient of thermal conductivity (TCK) from 25 °C to 100 °C, as shown in Eq. (3).

$$TCK = \frac{(k_{100^\circ\text{C}} - k_{25^\circ\text{C}})}{(100^\circ\text{C} - 25^\circ\text{C}) \times k_{25^\circ\text{C}}} \quad (3)$$

where $k_{100^\circ\text{C}}$ and $k_{25^\circ\text{C}}$ are the thermal conductivities of the specimens measured at 100 °C and 25 °C, respectively.

Fig. 6 shows the TCK of $(1-x)\text{MgSiO}_3-x\text{CaMgSi}_2\text{O}_6$ specimens sintered at 800 °C for 5 h. With increasing of $\text{CaMgSi}_2\text{O}_6$ content (x), the TCK of the specimens was increased up to $x = 0.46$ and then decreased. These results could be attributed to the change of crystalline phases from clino-enstatite to diopside (Fig. 3). Although the zero TCK is required for the stability of thermal conductivity, the large positive TCK is preferred to dissipate effectively the heat generated from LED chips of multi-chip packages. For

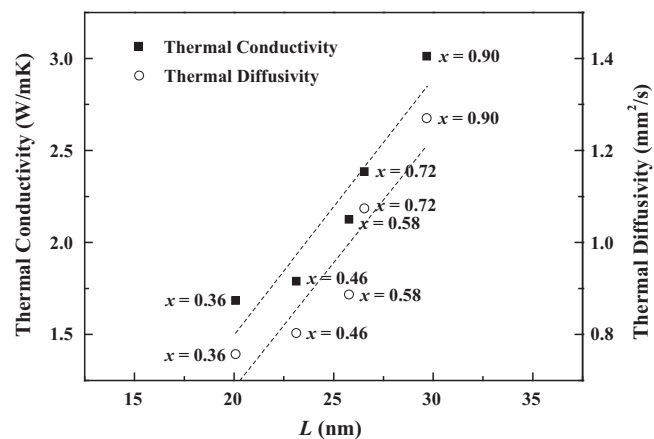


Fig. 5. Dependence of thermal conductivity and thermal diffusivity on average crystallite size (L) of $(1-x)\text{MgSiO}_3-x\text{CaMgSi}_2\text{O}_6$ specimens sintered at 800 °C for 5 h.

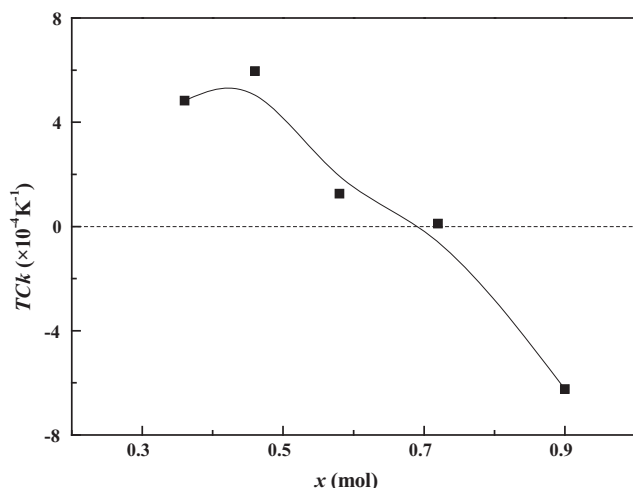


Fig. 6. Temperature coefficient of thermal conductivity (Tck) of $(1-x)\text{MgSiO}_3-x\text{CaMgSi}_2\text{O}_6$ specimens sintered at 800°C for 5 h.

$0.54\text{MgSiO}_3-0.46\text{CaMgSi}_2\text{O}_6$ specimens sintered at 800°C for 5 h, the highest Tck value of $5.96 \times 10^{-4}/K$ was obtained, which could be applicable to LED packages and substrates.

4. Conclusions

With increasing of $\text{CaMgSi}_2\text{O}_6$ content ($0.36 \leq x \leq 0.90$), the peak temperature of crystallization (T_p) of $(1-x)\text{MgSiO}_3-x\text{CaMgSi}_2\text{O}_6$ glasses was decreased, while the activation energy of crystallization (E_a) was increased up to $x = 0.58$ and then decreased. For the specimens sintered at 800°C for 5 h, the crystalline phases were changed from monoclinic clinoenstatite (MgSiO_3) to monoclinic diopside ($\text{CaMgSi}_2\text{O}_6$) with the $\text{CaMgSi}_2\text{O}_6$ content (x).

The specific heat capacity of the specimens was dependent on the E_a of glasses. With increasing of $\text{CaMgSi}_2\text{O}_6$ content (x), the thermal conductivity and thermal diffusivity of the specimens were increased due to the increase of crystallite size (L). The temperature coefficient of thermal conductivity (Tck) of the specimens was affected by the crystalline phases of

glass-ceramics. The highest Tck value of $5.96 \times 10^{-4}/K$ was obtained for $0.54\text{MgSiO}_3-0.46\text{CaMgSi}_2\text{O}_6$ specimens sintered at 800°C for 5 h.

Acknowledgements

This work was supported by the Human Resources Development of the Korea Institute of Energy Technology Evaluation and Planning (KETEP) grant funded by the Korea government Ministry of Knowledge Economy.

References

- [1] F. Nestola, G.D. Gatta, T.B. Ballaran, The effect of Ca substitution on the elastic and structural behavior of orthoenstatite, *American Mineralogist* 91 (2006) 809–815.
- [2] W.E. Lee, A.H. Heuer, On the polymorphism of enstatite, *Journal of the American Ceramic Society* 70 (1987) 349–360.
- [3] V.L. Balkevich, *Technical Ceramics*, Stroiizdat, Moscow, 1984 (in Russian).
- [4] M. Tribaudino, A transmission electron microscope investigation of the $C2/c \rightarrow P2_1/c$ phase transition in clinopyroxenes along the diopside-enstatite ($\text{CaMgSi}_2\text{O}_6-\text{Mg}_2\text{Si}_2\text{O}_6$) join, *American Mineralogist* 85 (2000) 707–715.
- [5] K. Matusita, S. Sakka, Kinetic study of crystallization of glass by differential thermal analysis-criterion on application of Kissinger plot, *Journal of Non-Crystalline Solids* 38–39 (1980) 741–746.
- [6] A. Goel, D.U. Tulyaganov, E.R. Shaaban, C.S. Knee, S. Eriksson, J.M.F. Ferreira, Structure and crystallization behaviour of some MgSiO_3 -based glasses, *Ceramics International* 35 (2009) 1529–1538.
- [7] A. Goel, D.U. Tulyaganov, V.V. Kharton, A.A. Yaremchenko, J.M.F. Ferreira, The effect of Cr_2O_3 addition on crystallization and properties of La_2O_3 -containing diopside glass-ceramics, *Acta Materialia* 56 (2008) 3065–3076.
- [8] H.E. Kissinger, Reaction kinetics in differential thermal analysis, *Analytical Chemistry* 29 (1957) 1702–1706.
- [9] R. Chen, Y. Wang, Y. Hu, Z. Hu, C. Liu, Modification on luminescent properties of $\text{SrAl}_2\text{O}_4:\text{Eu}^{2+}, \text{Dy}^{3+}$ phosphor by Yb^{3+} ions doping, *Journal of Luminescence* 128 (2008) 1180–1184.
- [10] Y.W. Kim, Y.W. Oh, S.Y. Yoon, R. Stevens, H.C. Park, Thermal diffusivity of reaction-sintered $\text{AlON}/\text{Al}_2\text{O}_3$ particulate composites, *Ceramics International* 34 (2008) 1849–1855.